An assessment of interface spaces for the accurate simulation of two-phase flows in high-contrast formations

Rafael T. Guiraldello[1], Franciane F. Rocha[2], Fabricio S. Sousa[2], Roberto F. Ausas[2], Gustavo C. Buscaglia[2], Felipe Pereira[3]

[1]*Piri Technologies, LLC*
1000 E. University Ave., 82071-2000, Laramie, WY, United States of America
rafaeltrevisanuto@gmail.com
[2]*Instituto de Ciências Matemáticas e de Computação, Universidade de São Paulo*
Av. Trabalhador São-carlense, 400, 13566-590, São Carlos, SP, Brazil
fr.franciane@usp.br, fsimeoni@icmc.usp.br, rfausas@icmc.usp.br, gustavo.buscaglia@icmc.usp.br
[3]*Department of Mathematical Sciences, The University of Texas at Dallas*
800 W. Campbell Road, 75080-3021, Richardson TX, United States of America
luisfelipe.pereira@utdallas.edu

Abstract. The design of accurate multiscale methods for the simulation of multiphase flows in channelized, high-contrast porous media remains as an important challenge in typical problems posed by the energy and environmental sectors. The Multiscale Robin Coupled Method (MRCM) [1] is a recently proposed multiscale domain decomposition method, that is a generalization of the Multiscale Mixed Method (MuMM) [2]. Such method ensures weak continuity of both normal fluxes and pressure for local problems with Robin boundary conditions, through low-dimensional interface spaces defined over the skeleton of a domain decomposition. The accuracy of the MRCM depends on the choice of the functions that span these interface spaces as well as on a Robin condition parameter. In this study we compare the accuracy of the MRCM in two-phase flow simulations with interface spaces spanned by: (i) piecewise polynomial functions; (ii) informed functions [3]; and (iii) physics-based functions [4]. We investigate the effect of such choices in approximating the saturation fields as well as the oil production curves for high-contrast channelized permeability fields. Numerical experiments indicate that the specialized interface spaces (ii) and (iii) have the potential to produce more accurate results by better accommodating the channelized features in comparison with standard polynomial functions.

Keywords: Porous Media, Multiscale Methods, Interface Spaces

1 Introduction

The design of accurate and efficient methods for the simulation of multiphase flows in channelized, high-contrast porous media is an important challenge for the approximation of problems posed by the energy and environmental sectors. The numerical solution of such problems must capture the heterogeneity of the porous medium. Depending on the level of details required and the size of the problem the model may have several billion cells and thousands of time steps, making the numerical simulations extremely expensive [5].

Multiscale methods have been introduced to provide accurate approximations at a reduced computational cost by decomposing large computational tasks in a family of smaller problems that can be solved simultaneously in parallel machines. This class of methods provides significant advances in the modeling of multiphase flow and transport problems in heterogeneous porous media, and has received considerable attention from several groups [6].

We consider the family of multiscale domain decomposition methods built in the Multiscale Robin Coupled Method (MRCM, [1]) to compute velocity fields for the simulations of two-phase flows in highly heterogeneous porous media. The MRCM is a recently proposed multiscale domain decomposition method, that is a generalization of the Multiscale Mixed Method (MuMM, [2]), the Multiscale Mortar Mixed Finite Element Method (MMM-

FEM, [7]), and the Multiscale Hybrid-Mixed Finite Element Method (MHM, [8]). Such method ensures weak continuity of both normal fluxes and pressure for local problems with Robin boundary conditions, through low-dimensional interface spaces defined over the skeleton of a domain decomposition. The accuracy of the MRCM depends on the choice of the functions that span these interface spaces as well as on a Robin condition parameter.

In this study, we consider an adaptivity strategy for setting the Robin parameter according to the permeability variations [9], and compare different strategies to define the interface spaces. The accuracy of the MRCM in two-phase flow simulations is investigated considering interface spaces spanned by: (i) piecewise polynomial functions; (ii) informed functions [3]; and (iii) physics-based functions [4]. Our multiscale numerical results are compared with fine grid solutions. We show the effect of such choices in approximating the saturation fields as well as the oil production curves for high-contrast channelized permeability fields. Numerical experiments indicate that the specialized interface spaces (ii) and (iii) have the potential to produce more accurate results by better accommodating the channelized features in comparison with standard polynomial functions.

2 The Multiscale Robin Coupled Method

The MRCM has been developed to find the Darcy velocity $\mathbf{u}(\mathbf{x})$ and the fluid pressure $p(\mathbf{x})$ describing flows in porous media, which (in the case of single-phase flow) are given by

$$\begin{aligned} \mathbf{u} &= -\kappa(\mathbf{x})\nabla p \quad && \text{in } \Omega \\ \nabla\cdot\mathbf{u} &= q && \text{in } \Omega \\ p &= g && \text{on } \partial\Omega_p \\ \mathbf{u}\cdot\mathbf{n} &= z && \text{on } \partial\Omega_u, \end{aligned} \tag{1}$$

where $\kappa(\mathbf{x}) = K(\mathbf{x})$ is the permeability tensor; q is a source term; g and z are the pressure and normal velocity boundary data, specified at boundaries $\partial\Omega_p$ and $\partial\Omega_u$, respectively ($\mathbf{n}$ is the outward unit normal). The domain Ω is decomposed into subdomains $\{\Omega_i\}_{i=1,\ldots,N}$, and the MRCM formulation consists in finding solutions $(\mathbf{u}_h^i, p_h^i)$ for each subdomain Ω_i, and global unknowns $(U_H, P_H) \in \mathcal{U}_H \times \mathcal{P}_H$ satisfying the local problems

$$\begin{aligned} \mathbf{u}_h^i &= -\kappa(\mathbf{x})\,\nabla p_h^i && \text{in } \Omega_i \\ \nabla\cdot\mathbf{u}_h^i &= q && \text{in } \Omega_i \\ p_h^i &= g && \text{on } \partial\Omega_i\cap\partial\Omega_p \\ \mathbf{u}_h^i\cdot\check{\mathbf{n}}^i &= z && \text{on } \partial\Omega_i\cap\partial\Omega_u \\ -\beta_i\mathbf{u}_h^i\cdot\check{\mathbf{n}}^i + p_h^i &= -\beta_i U_H\check{\mathbf{n}}\cdot\check{\mathbf{n}}^i + P_H && \text{on } \partial\Omega_i\cap\Gamma \end{aligned} \tag{2}$$

and compatibility conditions on the skeleton Γ (the union of all interfaces $\Gamma_{ij} = \Omega_i \cap \Omega_j$)

$$\sum_{i=1}^{N}\int_{\partial\Omega_i\cap\Gamma}(\mathbf{u}_h^i\cdot\check{\mathbf{n}}^i)\,\psi\,d\Gamma = 0 \quad \text{and} \quad \sum_{i=1}^{N}\int_{\partial\Omega_i\cap\Gamma}\beta_i(\mathbf{u}_h^i\cdot\check{\mathbf{n}}^i - U_H\,\check{\mathbf{n}}\cdot\check{\mathbf{n}}^i)\,\phi\,(\check{\mathbf{n}}\cdot\check{\mathbf{n}}^i)\,d\Gamma = 0, \tag{3}$$

for all $(\phi,\psi) \in \mathcal{U}_H \times \mathcal{P}_H$, where $\mathcal{U}_H$ and $\mathcal{P}_H$ are, respectively, the flux and pressure interface spaces defined over the edges of Γ. Here, $\check{\mathbf{n}}^i$ is the normal vector to Γ pointing outwards of Ω_i, and $\check{\mathbf{n}}$ is a fixed normal vector to Γ pointing outwards of Ω_1. The Robin condition parameter for the coupling of the subdomains is given by $\beta_i(\mathbf{x}) = \frac{\alpha(\mathbf{x})H}{\kappa_i(\mathbf{x})}$, where H is the characteristic size of the subdomains and $\alpha(\mathbf{x})$ is a dimensionless function defined according to the permeability variations.

The accuracy of the MRCM solution is mainly related to the Robin parameter β_i (see [9]) and to the functions that span the interface spaces $\mathcal{U}_H$ and $\mathcal{P}_H$. In this work, we compare the accuracy of the multiscale solutions produced by two distinct problem-dependent approximation spaces (or *informed spaces*) to those obtained with interface spaces spanned by piecewise polynomial functions. A brief description of how to build informed spaces are the subject of the next subsections.

2.1 Interface spaces based on SVD

The first procedure considered here is based on a two-step procedure: (i) construction of the so called *snapshot space* by retrieving traces of pressure and velocity solutions over Γ_{ij} on local Darcy-flow problems containing Γ_{ij}; (ii) selection of basis functions by applying a dimensional reduction technique (SVD in this study). The selected functions are defined over Γ and have support on Γ_{ij}. To make it precise, consider an interface $\Gamma_{i,j}$ and a region ω_k built, for example, as a collection of element such that $\Gamma_{i,j} \subset \omega_k$. In order to build the snapshot space for interface $\Gamma_{i,j}$ we solve $m = 1, \ldots, N$ local Darcy-flow problems on these oversampling regions ω_k, i.e.,

$$\begin{aligned} \mathbf{u}_h^{k,m} &= -K\nabla p_h^{k,m} && \text{in } \omega_k \\ \nabla \cdot \mathbf{u}_h^{k,m} &= C_{k,m} && \text{in } \omega_k \\ \mathcal{B}(\mathbf{u}_h^{k,m}, p_h^{k,m}; \beta^{k,m}) &= \delta_m(x) && \text{on } \partial\omega_k \end{aligned} \quad , \tag{4}$$

where $\mathcal{B}$ is a boundary operator which enforces either pressure, flux or Robin boundary conditions and $\delta_m(x)$ is a function that enforces data boundary condition and $C_{k,m}$ a the source term. After solving these problems, we retrieve the corresponding pressure and flux solution through the faces $e \in \Gamma_{ij}$ and end up with two column arrays $\underline{U}^{k,m}$ and $\underline{P}^{k,m}$ which are used to build the snapshot matrices

$$\begin{aligned} A_U^{\Gamma_{ij}} &= \left[\underline{U}^{k,1}, \ldots, \underline{U}^{k,N}\right], \\ A_P^{\Gamma_{ij}} &= \left[\underline{P}^{k,1}, \ldots, \underline{P}^{k,N}\right]. \end{aligned}$$

The next step is to perform the SVD decomposition on the two matrices above. After that, the first k_U and k_P left singular vectors are add to the basis of $\mathcal{U}_H$ and $\mathcal{P}_H$, respectively.

A comment is in order here: Although the MRCM allows to the use different spaces, a piecewise constant function with support on Γ_{ij} is added to the space $\mathcal{P}_H$ to ensure a globally conservative solution. In doing that we subtract the constant component of each column of $A_P^{\Gamma_{ij}}$, followed by the SVD decomposition. From that, we take the first $k_P - 1$ left singular vectors for the basis of $\mathcal{P}_H$ (see [3] for more details).

2.2 Interface spaces based on physics

Other choices for interface spaces besides classical polynomials are the new spaces based on the geometry of the heterogeneities [4], that are built to capture the variations of the solution caused by channelized features (such as high permeability channels and barriers). The physics-based basis functions for pressure are defined at the interfaces that contain high permeability channels and the physics-based basis functions for flux are set at the interfaces that contain barriers.

Let $[a, d]$ denote a line segment that is the support of an interface $\Gamma_{i,j} \subset \Gamma$ through which channelized structures pass. If a high-contrast channel passes in $[b, c] \subset [a, d]$, we define the following pressure basis functions:

$$\psi_1(x) = \begin{cases} \dfrac{b-x}{b-a} & \text{if } x \in (a,b) \\ 0 & \text{otherwise} \end{cases} \qquad \psi_2(x) = \begin{cases} \dfrac{x-a}{b-a} & \text{if } x \in (a,b) \\ 1 & \text{if } x \in (b,c) \\ \dfrac{d-x}{d-c} & \text{if } x \in (c,d) \end{cases} \qquad \psi_3(x) = \begin{cases} \dfrac{x-c}{d-c} & \text{if } x \in (c,d) \\ 0 & \text{otherwise.} \end{cases} \tag{5}$$

On the other hand, if a barrier passes in $[b, c] \subset [a, d]$, the flux basis functions are given by:

$$\phi_1(x) = \begin{cases} 1 & \text{if } x \in (a,b) \\ 0 & \text{otherwise} \end{cases} \qquad \phi_2(x) = \begin{cases} 1 & \text{if } x \in (b,c) \\ 0 & \text{otherwise} \end{cases} \qquad \phi_3(x) = \begin{cases} 1 & \text{if } x \in (c,d) \\ 0 & \text{otherwise.} \end{cases} \tag{6}$$

Both physics-based spaces can be defined simultaneously at the same interface, and the basis functions defined above can be easily extended to interfaces with more than one channelized structure. Linear polynomials are used at the interfaces without the presence of channelized features [4].

3 Two-phase flows

For two-phase flows of water and oil (denoted by w and o) in a fully saturated medium, the elliptic problem in eq. (1) is coupled with the following transport problem of water saturation (denoted by s)

$$\begin{aligned} \frac{\partial s}{\partial t} + \nabla \cdot (f(s)\mathbf{u}) &= 0 \quad \text{in } \Omega \\ s(\mathbf{x}, t=0) &= 0 \quad \text{in } \Omega \\ s(\mathbf{x}, t) &= 1 \quad \text{in } \partial\Omega^-, \end{aligned} \tag{7}$$

where $\mathbf{u} = \mathbf{u}(\mathbf{x}, t)$ and $\partial\Omega^- = \{\mathbf{x} \in \partial\Omega,\ \mathbf{u} \cdot \mathbf{n} < 0\}$ are the inlet boundaries. The function $f(s)$ is the fractional flow of water, given by $f(s) = \lambda_w(s)/\lambda(s)$, where $\lambda(s) = \lambda_w(s) + \lambda_o(s)$ is the total mobility. The mobility of each phase is given by $\lambda_j(s) = k_{rj}(s)/\mu_j$, where $k_{rj}(s)$ and μ_j, $j \in \{w, o\}$, are respectively the relative permeability and the viscosity of phase j. In this context, the conductivity in eq. (1) is given by $\kappa(\mathbf{x}) = \lambda(s(\mathbf{x}))K(\mathbf{x})$. The hyperbolic conservation law in eq. (7) is discretized by the upwind scheme (space) and the forward Euler method (time). The coupled system consisting of eqs. (1)-(7) is solved sequentially by an operator splitting technique [10].

4 Numerical experiments

In this section we present numerical experiments to compare the accuracy of the MRCM in two-phase flow simulations with different choices for the interface spaces. We use the relative permeability curves $k_{rw} = s^2$ and $k_{ro} = (1-s)^2$, a viscosity ratio of $\mu_o/\mu_w = 10$, and time expressed in PVI (Pore Volume Injected) [5]. The flow is established by imposing flux boundary conditions from left to right and no-flow at top and bottom in the domain $\Omega = [0,1] \times [0,1]$. No source terms are considered. A high-contrast permeability field containing high permeability channels and barriers is considered, see Fig. 1 (left). The background of the permeability field is given by $K(\mathbf{x}) = e^{4.5\xi(\mathbf{x})}$, where $\xi(\mathbf{x})$ is a self-similar Gaussian distribution having zero mean (truncated at short distances) and covariance function given by $C(\mathbf{x}, \mathbf{y}) = |\mathbf{x} - \mathbf{y}|^{-1/2}$ [11]. The permeability contrast is $K_{\max}/K_{\min} = 10^8$.

Concerning the MRCM, a computational grid with 64×64 fine grid cells equally divided into 4×4 subdomains is considered. We refer to the MRCM with the adaptive strategy [9] as aMRCM, and denote the combination of the aMRCM with the polynomial, informed spaces based on SVD, and physics-based spaces by aMRCM-POL, aMRCM-SVD, and aMRCM-PBS, respectively. The oversampling region ω_k for the informed spaces based on SVD is taken as a rectangular region that fits the interfaces in length and is built using the fine 4 grid cells closest to interface Γ_{ij} in both normal directions. The boundary operator imposes an inflow boundary condition with source term properly adjusted such that $\int_{\omega_k} C_{k,m} = \int_{\partial\omega_k} \delta_m$.

Figure 1 (center) shows the evolution in time of the relative errors for saturation considering as reference a solution produced by a fine grid solver. We compare the three choices for the interface spaces: piecewise polynomial, based on SVD, and physics-based. In the case of informed spaces based on SVD we consider a number of degrees of freedom per interface for each unknown equivalent to the polynomial spaces (linear for pressure and flux in this example). We note that the errors provided by the aMRCM-POL and aMRCM-SVD are comparable, while the errors delivered by the aMRCM-PBS are the smallest. The oil production curves are shown in Fig. 1 (right), where we note that the procedures that better predict oil production curves are the aMRCM-PBS and aMRCM-SVD. Note that the oil production curve computed by the aMRCM-POL differs considerably from the fine grid reference curve. Although the global errors of aMRCM-POL and aMRCM-SVD are comparable, when considering the production curves, it is possible to spot a huge improvement for the latter.

A comparison of the saturation profiles can be found in Fig.2, where we note that the more accurate solutions are yielded by the aMRCM-SVD and aMRCM-PBS. Therefore, the design of the pressure and flux basis functions has a large impact on the transport of the water saturation.

Next, we add more degrees of freedom to the aMRCM-POL and aMRCM-SVD approximations. Figure 3 shows the saturation errors (left) and oil production curves (right) provided by the aMRCM-POL and aMRCM-SVD considering $(k_U, k_P) = (2,2)$, $(k_U, k_P) = (3,3)$, $(k_U, k_P) = (4,4)$, and $(k_U, k_P) = (5,5)$. We note that to recover an error similar to the produced by the aMRCM-PBS, polynomials of the fourth order are needed. The errors of the aMRCM-POL drop when higher dimensional interface spaces are used, while the aMRCM-SVD does not benefit from the increase in the number of degrees of freedom, for this example. The same observation can be drawn from the oil production curves as well as from the saturation profiles illustrated in Fig. 4.

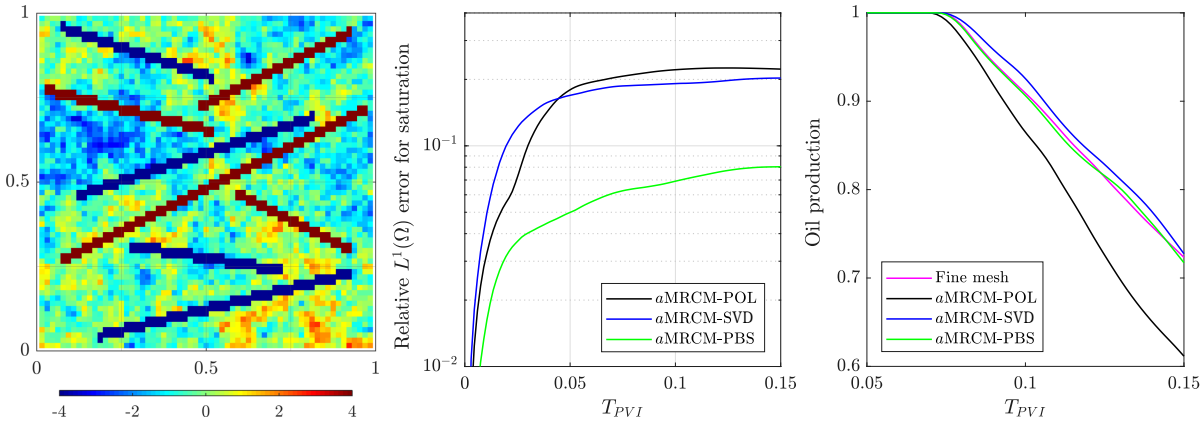

Figure 1. Log-scaled permeability field (left), saturation errors (center), and oil production curves (right).

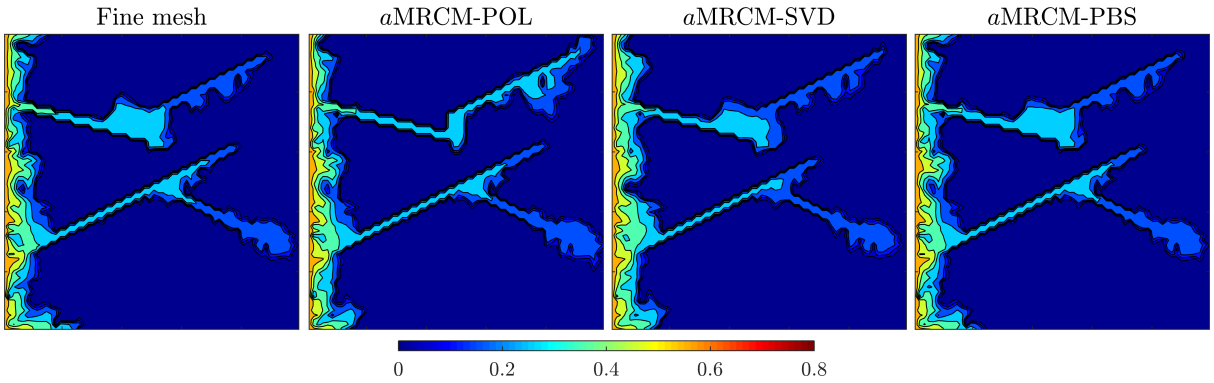

Figure 2. Saturation profiles.

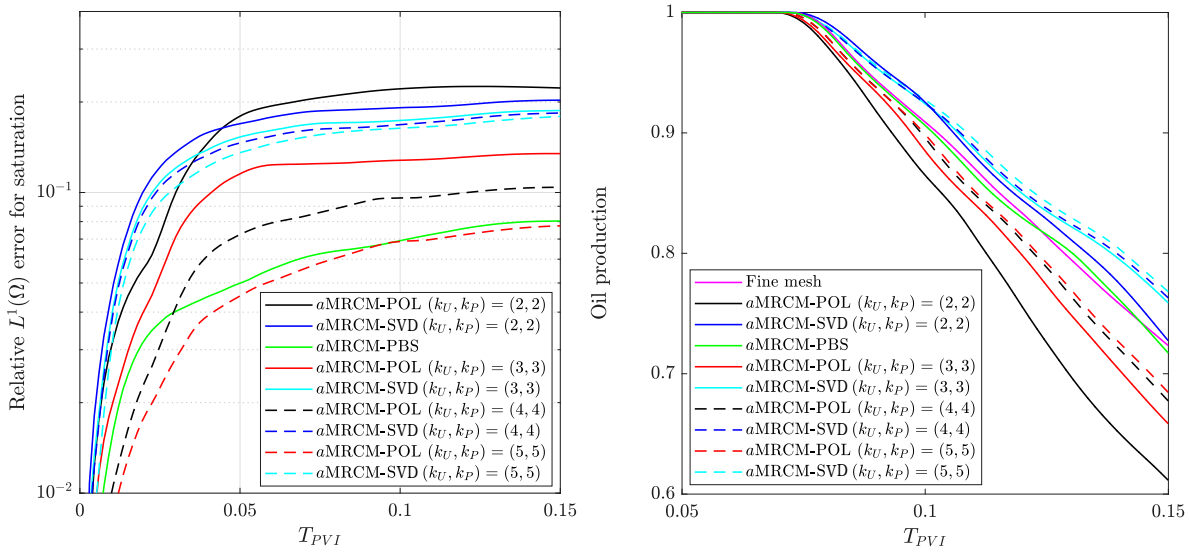

Figure 3. Saturation errors (left) and oil production curves (right).

We show in Table 1 the number of interface unknowns required by all the interface spaces considered. An average value for the number of degrees of freedom per interface is presented for the aMRCM-PBS since it may be different on each interface depending locally on the permeability field. If we consider the least expensive

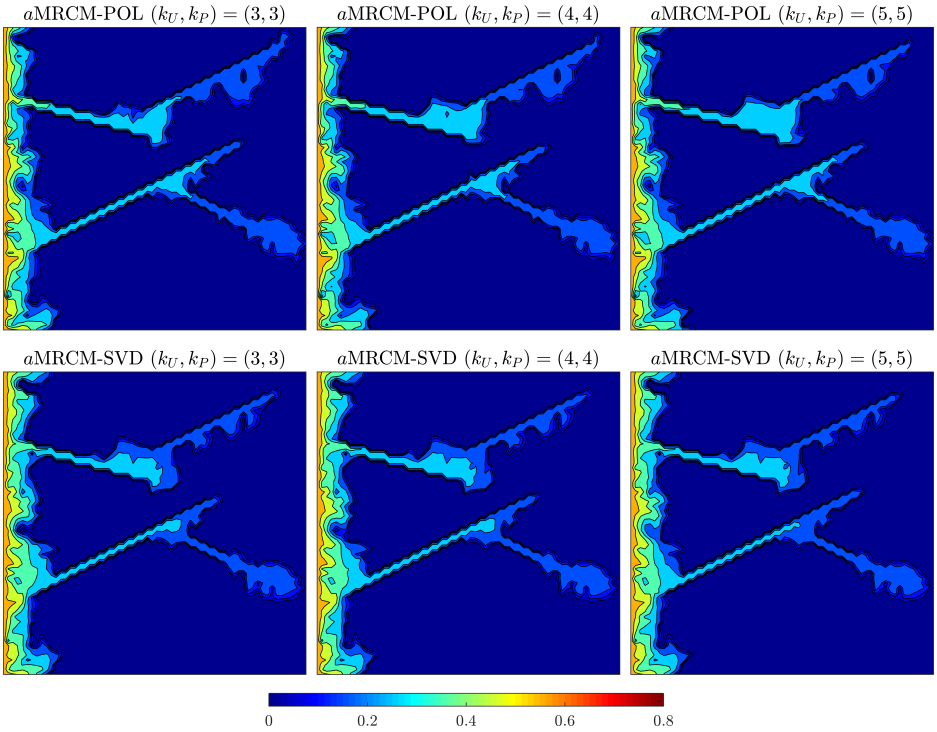

Figure 4. Saturation profiles produced by the aMRCM-POL and aMRCM-SVD with different degrees of freedom.

choices in terms of degrees of freedom, that are the most attractive options from the point of view of computational efficiency [12], we note that the aMRCM-SVD with $(k_U, k_P) = (2, 2)$ and the aMRCM-PBS have the best potential to produce more accurate results by better accommodating the channelized features in comparison with the aMRCM-POL with $(k_U, k_P) = (2, 2)$. Note that among all the interface spaces considered in Fig. 3 and Table 1, the aMRCM-PBS is the one that provides the best balance between precision and number of interface unknowns, and hence, computational cost. Therefore, we conclude that the specialized interface spaces are able to offer improved accuracy in comparison with the standard polynomial spaces in the presence of high-contrast channelized structures, while keeping efficient simulations.

Table 1. Number of interface unknowns required by the interface spaces.

Interface space	*Dof's* per interface	Total of interface unknowns
aMRCM-POL and aMRCM-SVD	$(k_U, k_P) = (2, 2)$	96
aMRCM-POL and aMRCM-SVD	$(k_U, k_P) = (3, 3)$	144
aMRCM-POL and aMRCM-SVD	$(k_U, k_P) = (4, 4)$	192
aMRCM-POL and aMRCM-SVD	$(k_U, k_P) = (5, 5)$	240
aMRCM-PBS	$(k_U, k_P) \approx (2.29, 2.04)$	104

5 Conclusions

The MRCM not only generalizes other multiscale mixed methods but also shows improved accuracy for highly heterogeneous porous media flows. With the combination of its Robin parameter adaptivity and the specialized interface spaces (informed spaces based on SVD and physics-based spaces), we achieve considerably improvement in accuracy in the approximation of two-phase flows when compared to the classic polynomial spaces. We remark that other multiscale solvers can take advantage of the developments reported in this work since the interface spaces considered here can be extended to different multiscale methods in a straightforward manner.

Future works include the extension of the interface spaces to the 3D scenario. In the case of the informed

spaces such extension is immediate by replacing the local boundary operators in 2D with their version in 3D. On the other hand, the construction of automatized physics-based spaces in 3D requires new developments, which are currently being considered by the authors.

Acknowledgements. We acknowledge the financial support from Petrobras (grant 2015/00400-4), FAPESP (grant CEPID-CeMEAI 2013/07375-0), CNPq (grants 305599/2017-8 and 310990/2019-0), and CAPES (Code 001).

Authorship statement. The authors hereby confirm that they are the sole liable persons responsible for the authorship of this work, and that all material that has been herein included as part of the present paper is either the property (and authorship) of the authors, or has the permission of the owners to be included here.

References

[1] R. T. Guiraldello, R. F. Ausas, F. S. Sousa, F. Pereira, and G. C. Buscaglia. The multiscale Robin coupled method for flows in porous media. *Journal of Computational Physics*, vol. 355, pp. 1–21, 2018.
[2] A. Francisco, V. Ginting, F. Pereira, and J. Rigelo. Design and implementation of a multiscale mixed method based on a nonoverlapping domain decomposition procedure. *Mathematics and Computers in Simulation*, vol. 99, pp. 125–138, 2014.
[3] R. T. Guiraldello, R. F. Ausas, F. S. Sousa, F. Pereira, and G. C. Buscaglia. Interface spaces for the multiscale Robin coupled method in reservoir simulation. *Mathematics and Computers in Simulation*, vol. 164, pp. 103–119, 2019.
[4] F. F. Rocha, F. S. Sousa, R. F. Ausas, F. Pereira, and G. C. Buscaglia. Interface spaces based on physics for multiscale mixed methods applied to flows in fractured-like porous media. *Computer Methods in Applied Mechanics and Engineering*, vol. 385, pp. 114035, 2021.
[5] Z. Chen, G. Huan, and Y. Ma. *Computational methods for multiphase flows in porous media*, volume 2. SIAM, 2006.
[6] V. Kippe, J. Aarnes, and K. Lie. A comparison of multiscale methods for elliptic problems in porous media flow. *Computational Geosciences*, vol. 12, n. 3, pp. 377–398, 2008.
[7] T. Arbogast, G. Pencheva, M. Wheeler, and I. Yotov. A multiscale mortar mixed finite element method. *Multiscale Modeling & Simulation*, vol. 6, n. 1, pp. 319–346, 2007.
[8] C. Harder, D. Paredes, and F. Valentin. A family of multiscale hybrid-mixed finite element methods for the Darcy equation with rough coefficients. *Journal of Computational Physics*, vol. 245, pp. 107–130, 2013.
[9] F. F. Rocha, F. S. Sousa, R. F. Ausas, G. C. Buscaglia, and F. Pereira. Multiscale mixed methods for two-phase flows in high-contrast porous media. *Journal of Computational Physics*, vol. 409, pp. 109316, 2020.
[10] J. Douglas, F. Furtado, and F. Pereira. On the numerical simulation of waterflooding of heterogeneous petroleum reservoirs. *Computational Geosciences*, vol. 1, n. 2, pp. 155–190, 1997.
[11] F. Futado, J. Glimm, W. B. Lindquist, and F. Pereira. Characterization of mixing length growth for flow in heterogeneous porous media. In *SPE Symposium on Reservoir Simulation*. OnePetro, 1991.
[12] A. Jaramillo, R. T. Guiraldello, S. Paz, R. F. Ausas, F. S. Sousa, F. Pereira, and G. C. Buscaglia. Towards HPC simulations of billion-cell reservoirs by multiscale mixed methods. *arXiv preprint arXiv:2103.08513*, vol. , 2021.